JOURNAL OF SOLID STATE CHEMISTRY 72, 209–217 (1988)

Study by Electrical Conductivity of the Process of Oxidation and of the Change of Structure in Synthetic Titanomagnetites

B. GILLOT AND F. JEMMALI

Laboratoire de Recherches sur la Réactivité des Solides associé au CNRS, Faculté des Sciences Mirande, B.P. 138, Dijon Cedex 21004, France

AND A. ROUSSET

Laboratoire de Chimie des Matériaux Inorganiques, Université Paul Sabatier, Toulouse III 118, route de Narbonne, Toulouse Cedex 31062, France

Received December 22, 1986; in revised form April 22, 1987

During oxidation in air of submicronic synthetic titanomagnetites $(Fe^{2+}_{1+x}Fe^{3+}_{2-2x}Ti^{4+}_{x})O^{2-}_{4}$ $(0 < x < 0.82)$ the temperature dependence of the electrical conductivity over a temperature range 300–1000 K was investigated. Below 700 K the titanomagnetites are oxidized in cation deficient spinels and the evolution of electrical conductivity might be closely associated with the position and the oxidation degree of iron cations in the spinel lattice. The profile of the $\sigma = f(t)$ curves shows that the mechanism of electrical conduction can be related to the electronic exchange between the Fe^{2+} and Fe^{3+} ions in octahedral as well as tetrahedral positions of the spinel lattice. Above 700 K, the electrical conductivity yields discontinuities in the $\log \sigma = (f(1/T)$ curves attributed to the generation of new phases of α-Fe_2O_3, TiO_2, and Fe_2TiO_5. Titanium does not appear to have a stabilizing effect on the phase change.

Introduction

In this paper we report the results of our attempt to use electrical conductivity to characterize the process of oxidation of finely grained titanomagnetites $Fe_{3-x}Ti_xO_4$ $(0 < x < 0.82)$. Previously, it was shown that these spinels containing iron(II), whose crystallite sizes are less than 100 nm, could be oxidized to defect phase γ with the same spinel structure (cation deficient spinels known generically as titanomaghemites) at temperature <700 K. From thermogravimetric data (*1*) it was found that the diffusion rates of ions in the two sublattices of the spinel structure are not equal and that consequently the availability for oxidation of Fe^{2+} ions in tetrahedral sites (A sites) is much less than that for Fe^{2+} ions in octahedral sites (B sites). This results in a two-stage reaction in which tetrahedrally sited Fe^{2+} ion is only oxidized after octahedrally sited Fe^{2+} ion reacts (*2–5*); this information has been used to determine the iron cation distributions between the sublattices (*1*). Moreover, titanomaghemites are metastable above about 740 K and a systematic study of the decomposition of these cation deficient spinels has recently been made by IR spectroscopy (*6*). Infrared spectra re-

0022-4596/88 $3.00

TABLE I

CATION DISTRIBUTIONS AND PHYSICAL PROPERTIES IN UNOXIDIZED $Fe_{3-x}Ti_xO_4$

x	Sample composition	Crystallite size (nm)	Lattice parameter (nm)	T_c (K)
0.20	$(Fe^{3+})_A(Fe^{3+}_{0.6}Fe^{2+}_{1.20}Ti^{4+}_{0.20})_BO_4^{2-}$	100	0.8405	754
0.61	$(Fe^{3+}_{0.70}Fe^{2+}_{0.30})_A(Fe^{3+}_{0.01}Fe^{2+}_{1.38}Ti^{4+}_{0.61})_BO_4^{2-}$	70	0.8467	515
0.82	$(Fe^{3+}_{0.20}Fe^{2+}_{0.80})_A(Fe^{3+}_{0.05}Fe^{2+}_{1.13}Ti^{4+}_{0.82})_BO_4^{2-}$	90	0.8516	324

vealed that inversion products of highly oxidized compositions may contain hematite (α-Fe_2O_3), rutile (TiO_2), and pseudobrookite (Fe_2TiO_5).

Because of the possibility of electron "hopping" between Fe^{2+} and Fe^{3+} ions which may occur at octahedral sites as well as tetrahedral sites for these spinels containing iron cations of variable valency and because electrical conductivity is also a sensitive physical technique to study the phase changes (*7*), an investigation of the electrical behavior was undertaken to understand the physical and chemical changes occurring during the oxidation in synthetic titanomagnetites over the temperature range 300 to 1000 K. The only attempt that has been made to study the electrical properties of oxidized titanomagnetites (*8*) was achieved by oxidizing natural titanomagnetites separated from tertiary and quaternary igneous rocks. However, in such specimens appreciable amounts of other cations and a wide range in grain size might change the oxidation mechanism.

Samples—Experimental

The conditions of preparation of finely grained titanomagnetites and of characterization (differential thermal analysis, X-ray analysis, specific area, chemical analysis, morphology) have already been published in (*1, 6*). The thermal decomposition of mixed iron titanium oxalates leads, through appropriate thermal treatments at low temperature (<700 K), to the solid solutions ($Fe_3O_{4(1-x)}Fe_2TiO_{4(x)}$) which are extremely finely divided solids and hence very reactive. The samples consist of almost spherical grains with an average diameter in the range between 70 and 100 nm (Table I). X-ray crystallographic analysis shows that the samples contain only the spinel phase with a lattice parameter which increases with x (Table I) and the cation distribution determined by thermogravimetry (*1*) is mentioned in Table I. In this procedure, the Fe^{2+}(B) and Fe^{2+}(A) concentrations versus composition x are calculated from the $\Delta m_B/\Delta m_{oexp}$ and $\Delta m_A/\Delta m_{oexp}$ ratios, where Δm_B and Δm_A represent the values of the weight gain for each site and Δm_{oexp} is the weight gain for pure magnetite. The distribution of Fe^{2+} ions on B and A sites given in Table I approaches that deduced at low temperature (300 K) by Trestman-Matts *et al.* (*9*) using thermoelectric coefficient measurements and by Wechsler *et al.* (*10*) which indicates that no Ti^{4+} resides tetrahedrally.

Until now, the method selected to produce laboratory titanomagnetites in the form of small grains (<1 μm) had in general been performed by the ball milling in water of sintered samples obtained by the ceramic method (at 1450 K) and prepared from α-Fe_2O_3 and TiO_2 (*11, 12*). Under these conditions, it is difficult to obtain homogeneous grains without absorbed water remaining after grinding. The presence of absorbed water through wet grinding seems to provide an oxygen source and in this

case it soon becomes apparent that the amount of oxidation is not particularly sensitive to the atmosphere since the samples can remain oxidized in an atmosphere of flowing hydrogen (*12*).

In our case the samples were oxidized in air ($P_{O_2} = 2 \times 10^4$ Pa) isothermally in the conductivity apparatus, or the temperature was increased at a linear rate from room temperature to 1000 K. The dc conductivity was measured point by point by means of a two-probe device on compressed pellets as reported in Ref. (*13*). Before each experiment great care had to be taken during heat treatment in the cell (1000 K for 1 hr in a flow-through N_2 atmosphere) to ensure that the powder was not partially oxidized and that other phases (for example, $FeTiO_3$, FeO) did not appear. Under these conditions to check for oxidation during the thermal treatment process, heating samples were X-rayed and in all cases the lattice parameters agreed very well with those of the initial specimens indicating that no oxidation was present. In N_2 atmosphere, the compounds in all cases exhibit semiconducting behavior with a change in the slope of log σT vs $1/T$ curves which may be attributed to a Curie temperature (noted T_c in Table I) as observed for iron–zinc, iron–cobalt, or iron–manganese ferrites in the vicinity of the Curie point (*14–16*). It is known that the slope of the log σT vs $1/T$ curve changes at the Curie point and that the conductivity activation energy increases on passing from the ferrimagnetic (E_f) to the paramagnetic (E_p) phase. The T_c values agree reasonably well with the results of Ref. (*12*). However, Hauptman (*17*) pointed out that for unoxidized titanomagnetites with $x = 0.60$, T_c is about 440 K whereas the reported value of 515 K (Table I) for the same composition must indicate an oxidation. The most reasonable explanation involves differences in titanomagnetite preparation techniques to produce fine-grained samples and in impurity concentrations. In particular, as mentioned in Ref. (*18*), titanium clustering appears to be characteristic of the sintering process and the formation of iron-rich regions could account for differences in Curie temperature. The intermediate phases present after oxidation were determined by X-ray powder diffraction from samples rapidly cooled from various temperatures in the cell.

Results

The effect of temperature on oxidation characteristics was demonstrated directly by observing the plots of log σ vs $1/T$ when samples of different compositions ($x = 0.20$, $x = 0.61$, and $x = 0.82$) were heating in air at a constant rate of 3 K min^{-1} from room temperature to 1000 K (regions I and II, Fig. 1). In region I and for samples heating at 1 K min^{-1} (Fig. 2), the conductivity increases up to 470 K giving a maximum at about 460 K for $x = 0.20$ and $x = 0.61$ (curves a and b) and two maxima at 515 and 590 K for $x = 0.82$ (curve c). Then, the spinels undergo a large conductivity decrease during further oxidation until the sample transforms to nonstoichiometric titanomagnetites with a δ value approaching unity (point A, Fig. 1) related to the genera-

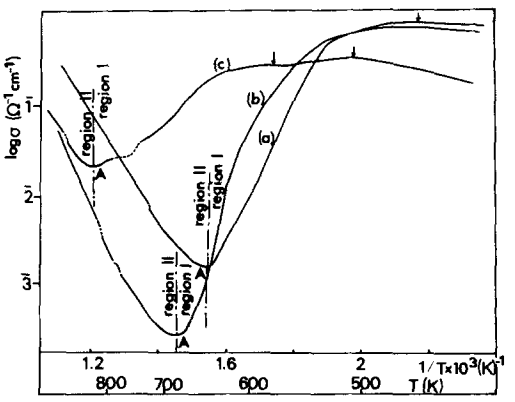

FIG. 1. Behavior of electrical conductivity of titanium-substituted magnetites heated in air at 3 K/min. (a) $x = 0.20$; (b) $x = 0.61$; (c) $x = 0.82$.

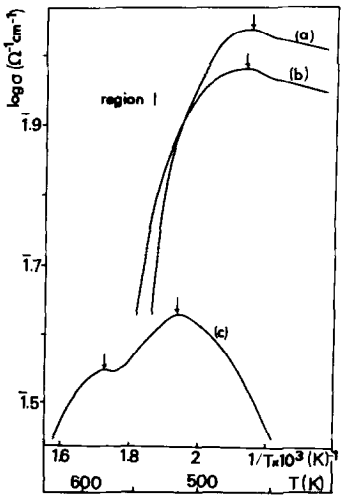

FIG. 2. Log $\sigma = f(1/T)$ curves showing conductivity maxima (indicated by arrows) in region I during progressive oxidation of titanomagnetites. (a) $x = 0.20$; (b) $x = 0.61$; (c) $x = 0.82$. Heating rate: 1 K/min.

tion of Fe^{3+} ions and vacancies (□) (*19*) in the spinel lattice according to 3 $Fe^{2+} \rightarrow 2$ Fe^{3+} + □. However, for $x = 0.82$, the conductivity decreases slowly and a discontinuity is observed at around 740 K

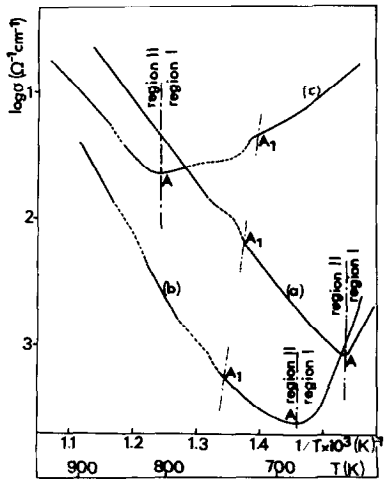

FIG. 3. Log $\sigma = f(1/T)$ curves showing the discontinuities (represented in dashed lines) during the phase transformation. (a) $x = 0.20$; (b) $x = 0.61$; (c) $x = 0.82$. Heating rate: 1 K/min.

before point A (noted A_1 in Fig. 3) although X-ray analysis confirmed that at this temperature a single-phase cation deficient spinel was formed (curve a, Fig. 4). In addition, the minimum (point A) is shifted toward higher temperatures with increased titanium substitution (Fig. 3). After oxidation of the samples, superstructure lines were found indicating a 5 : 1 and, in some cases, possibly a 3 : 1 order of cations and vacancies (*20*).

The decrease in σ is then followed by an increase in σ (region II, Fig. 3) but for all compositions this evolution is not completely linear and one or two breaks (repre-

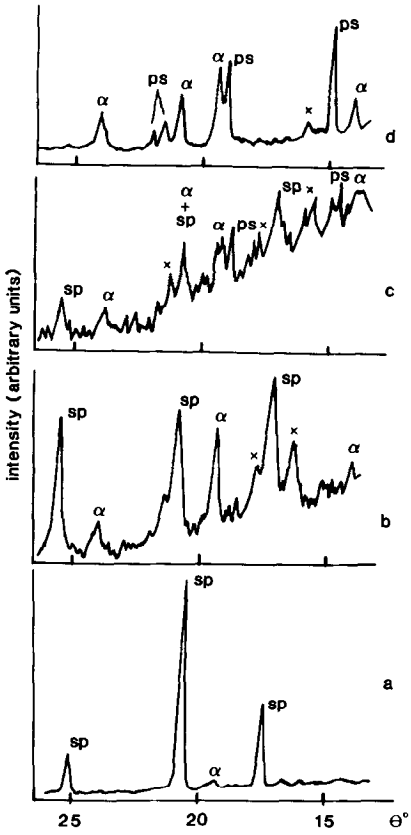

FIG. 4. X-ray powder diffraction pattern during oxidation at different temperatures of a sample with $x = 0.82$ and oxidized at (a) 740 K, (b) 810 K, (c) 870 K, (d) 973 K. sp, spinel; x, TiO_2; α, α-Fe_2O_3; ps, pseudobrookite.

sented by dashed lines as in region I) can be distinguished. These breaks can be regarded as being caused by structural changes (*7*) or as due to chemical decomposition (*21*). During an examination of the powder diffraction pattern of the sample heated above 800 K (Fig. 4) a large number of lines were observed in contrast to the few lines of the spinel structure. Some of the lines can be identified with those of α-Fe_2O_3 for $x \simeq 0.20$, whereas for $x = 0.61$ and $x = 0.82$ a whole series of other phases is generated: titanomaghemite, α-Fe_2O_3, TiO_2 at a temperature of 810 and 870 K (curves b and c, Fig. 4), and α-Fe_2O_3 and pseudobrookite Fe_2TiO_5 above 900 K (curve d, Fig. 4).

Discussion and Conclusion

One interesting result from this study is that single-phase cation deficient spinels were formed in air for temperatures <700 K. It has been shown (*22*) that the oxidation process produces homogeneous grains of titanomaghemites with vacancies uniformly distributed throughout the grain bulk for different values of x and δ (δ = oxidation degree) probably because of the smaller grain sizes resulting from the preparation method at low temperature. The X-ray peaks and the lattice parameters of partially or totally oxidized fine-grained samples with a high surface area indicated that the titanomaghemites have homogeneously oxidized, which is important for understanding the electrical behavior in relation to cation distribution. This is similar to the results of Keefer and Shive (*12*) concerning the production of synthetic titanomaghemites with no oxidation gradients. Also, the majority of studies made on titanomagnetites produced from sintered samples did not agree with these results because of the formation of inhomogeneously oxidized grains which depend upon crystallite size (*23*).

It has been established from kinetic studies that the oxidation process is controlled by a law of diffusion, under variable working conditions, of the vacancies generated at the solid–gas interface. The B site Fe^{2+} ions will be oxidized more rapidly than A site Fe^{2+} ions as ions in B sites are ionically bound whereas those in A sites are more strongly bound due to covalency. The two maxima at 515 and 590 K for $x = 0.82$ probably represent the two stages of oxidation. In order to discriminate the reactivity of tetrahedral and octahedral ferrous ions, the formation of cation deficient titanomagnetites was also followed by observing the time dependence of electrical conductivity at an oxygen pressure of 3.30×10^3 Pa. For the three compositions, the plots of σ versus time at constant temperature between 400 and 530 K (Fig. 5) exhibit a maximum related to the oxidation of Fe^{2+} ions located at B sites. It is known that the octahedral sites favor electron exchange between Fe^{2+} and Fe^{3+} ions and Fe^{2+} ions on B sites are initially more numerous than those on A sites (Table I) and are oxidized preferentially (*1*). Then, versus time, the

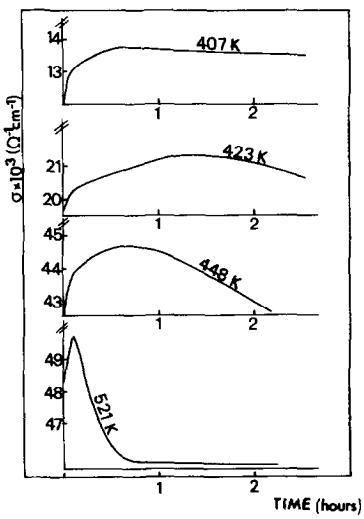

FIG. 5. Oxidation isotherm of Fe^{2+} ions located at B sites for composition $x = 0.82$ and for $T < 550$ K.

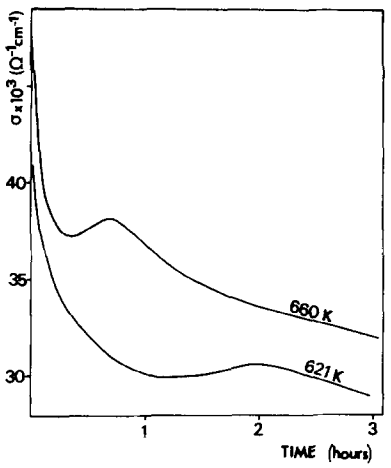

FIG. 6. Oxidation isotherm of Fe^{2+} ions located at A sites for composition $x = 0.82$ and for $T > 600$ K.

conductivity decreases related to the generation of Fe^{3+} ions and vacancies on B sites. Pure magnetite ($x = 0$), with a high initial conductivity (Fe^{2+} and Fe^{3+} ions initially present in equal amounts), always undergoes a large conductivity decrease during oxidation.

For $x = 0.82$, the conductivity reaches a stable level at about 520 K (curve d, Fig. 5) which can be regarded as being caused by the total oxidation of Fe^{2+} ions on B sites. Thus, in this temperature range and for this composition only a part of the total Fe^{2+} ions is readily oxidized and some Fe^{2+} ions (those located on A sites) remain unoxidized, becoming oxidized at higher temperatures. In order to analyze the effect of this oxidation, the evolution of electrical conductivity σ vs time is shown in Fig. 6 for temperatures above 600 K. It can be seen that the conductivity decreases initially (due to the oxidation of Fe^{2+} ions on B sites) against time and then exhibits a maximum. The presence of Fe^{2+} ions at A sites appears to provide an explanation for the fact that the conductivity undergoes a maximum. This is due to the simultaneous presence of Fe^{2+} and Fe^{3+} ions on A sites which allows electron exchange between cations on equivalent sites. Indeed, electron hopping between tetrahedral sites contribute to the conductivity of certain ferrites, and has an activation energy of 0.2 to 0.3 eV (*24*). This is considerably smaller than the observed activation energy of the oxidation reaction (~1.3 eV) (*1*), and electron hopping should therefore make an effective contribution to the process. When the amount of Fe^{3+} ions becomes large, the electronic exchange is upset and the conductivity decreases. For $x = 0.61$, we observe no maximum because there are initially fewer Fe^{2+} ions in A sites than Fe^{3+} ions.

From these results it is possible to conclude that the electrical conductivity will be governed by the initial cation distribution. If the degree of oxidation of the titanomagnetite $(Fe^{2+}_{1+x}Fe^{3+}_{2-2x}Ti^{4+}_{x})O^{2-}_{4}$ is defined by an oxidation parameter δ given by the reaction

$$Fe^{2+} + (\delta/2)O \rightarrow \delta Fe^{3+} + (1 - \delta)Fe^{2+} + (\delta/2)O^{2-} \quad (1)$$

and on the assumption that Ti^{4+} ions and vacancies are located only in octahedral sites, the number of Fe^{2+} ions and of vacancies per molecule would be, respectively,

$$\frac{8(1 - \delta)(1 + x)}{8 + \delta(1 + x)} \quad \text{and} \quad \frac{3\delta(1 + x)}{8 + \delta(1 + x)}. \quad (2)$$

The cation distribution, after partial oxidation of Fe^{2+} ions on B sites, may then be written

$$[Fe^{3+}_{1-z}Fe^{2+}_{z}]_{A} \left[Fe^{2+}_{8(1-\delta)(1+x)/(8+\delta(1+x))-z} Fe^{3+}_{8(2-2x+\delta)(1+x)/(8+\delta(1+x))+z-1} \cdot Ti^{4+}_{8x/(8+\delta(1+x))}\square_{3\delta(1+x)/(8+\delta(1+x))}\right]_{B}O^{2-}_{4}, \quad (3)$$

where z is the number of unoxidized Fe^{2+} ions on A sites and $\square$ denotes vacancies. From the arguments already given, z will remain constant as oxidation proceeds in B sites and the cation distribution in B sites is therefore completely described by x and δ.

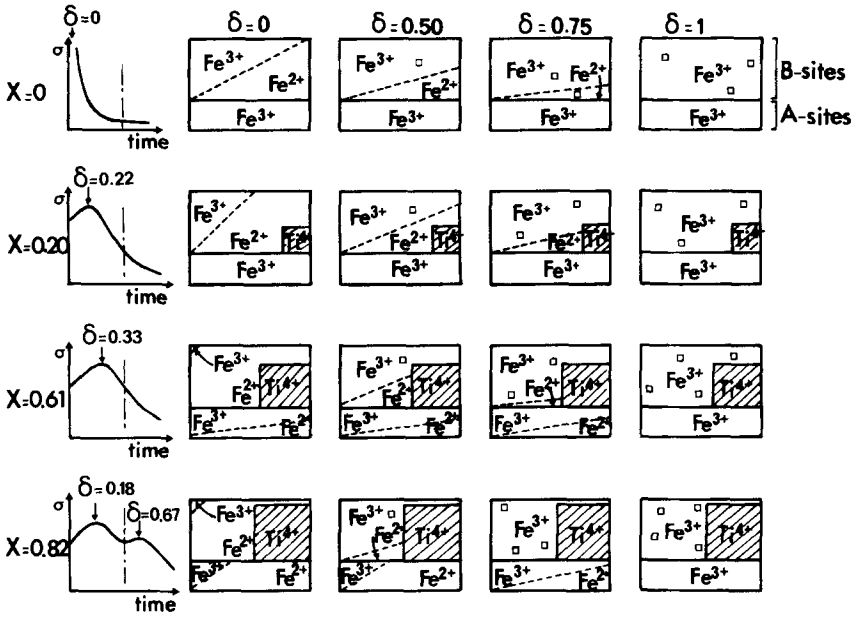

FIG. 7. Schematic representations of the various Fe^{2+}–Fe^{3+} "hopping" possibilities on B and A sites as functions of x and δ, □, cation vacancy. For each composition, we have represented the scheme of the evolution of σ vs time. The arrows indicate the theoretical values of δ for which the amounts of Fe^{2+} and Fe^{3+} ions on B or A sites are equivalent. The pure magnetite ($x = 0$) is given for comparison.

Figure 7 shows the various possibilities of electronic exchange between Fe^{2+} and Fe^{3+} ions as a function of x and δ. For $\delta < 0.5$ and for all compositions, the Fe^{2+} ions in A sites are not oxidized and the maximum conductivity obtained at low temperature (<550 K), as observed experimentally (Fig. 5), can be attributed to the oxidation of Fe^{2+} ions located on B sites. Theoretically, this maximum of conductivity appears when the amounts of Fe^{2+} and Fe^{3+} ions are equivalent. Calculation of δ for which the amounts of Fe^{2+} and Fe^{3+} ions on B sites are equivalent may be made from the cation distribution given in Table I using Eq. (*3*). The results of this calculation are respectively $\delta = 0$ for $x = 0$, $\delta = 0.22$ for $x = 0.20$, $\delta = 0.33$ for $x = 0.61$, and $\delta = 0.18$ for $x = 0.82$ (Fig. 7). When all the Fe^{2+} ions have been oxidized ($\delta > 0.5$) the reaction can only proceed by the oxidation of A ions, resulting for the composition $x = 0.82$ of a second maximum (Fig. 6) because Fe^{2+} ions in A sites are initially more numerous than Fe^{3+} ions. This maximum of σ results when the Fe^{2+} and Fe^{3+} on A sites are equal in concentration, i.e., $\delta = 0.67$ (Fig. 7). One must, however, also consider that, in the study by Schmidbauer (*25*) using Mössbauer spectroscopy on cation deficient Fe_2TiO_4, a small amount of tetrahedral vacancies (about 20%) may slightly modify the δ value at maximum, particularly for high degrees of oxidation.

Although the availability for oxidation of Fe^{2+} ions in A sites is much lower than that in B sites, the oxidation of A site Fe^{2+} ions allows the retention of the original spinel structure without the formation of multiphase oxidation products over the range of composition $0 < x < 0.7$ since the presence of other phases would imply a discontinuity in plots of log σ vs $1/T$ before the point A (*7*). At this point the oxidation is complete

($\delta = 1$). For $x = 0.82$, completely oxidized titanomagnetite cannot be obtained without a rhombohedral phase since the plot of log σ vs $1/T$ shows a discontinuity before the point A. For $x = 0.82$, in fact, the entire range $0 < \delta < 0.80$ was accomplished without the presence of a rhombohedral phase as confirmed by X-ray diffraction. The implication of this result is that the second maximum in the $\sigma = f(t)$ (Fig. 6) which appears at about $\delta = 0.67$ corresponds to a nonstoichiometric titanomagnetite.

X-ray analysis indicated that single-phase cation deficient spinels were obtained up to point A_1 (Fig. 3) which can be considered as the onset of the phase change. Figure 3 shows that the titanomaghemite inversion temperature is not consistently influenced by titanium content, as the point A is little displaced with x; thus, titanium has no apparent effect on the stability of the titanomaghemite lattice although for the titanomaghemite with $x = 0.61$ and $\delta = 1$ (curve b, point A_1) we observe a small increase in transformation temperature (740 K for $x = 0.61$ and 724 K for $x = 0.20$) as confirmed by differential thermal analysis. Keefer and Shive (*26*) also noted that titanium does not appear to stabilize the spinel structure, which is consistent with our finding. Vacancies, on the other hand, do appear to have a stabilizing effect since titanomaghemite with $x = 0.61$ (0.50 vacancy per molecule) is more stable than the titanomaghemite with $x = 0.20$ (0.39 vacancy per molecule). However, in the present case, the effect of particle size (Table I) may explain the increase in stability. Previously, it has been found for the γ-$Fe_2O_3 \rightarrow \alpha$-$Fe_2O_3$ transformation (*7*) that the reduced particle size facilitates the release of strain which increases the transformation temperature.

At elevated temperatures in air the nature of the transformation products depends upon the composition of the cation deficient spinels. α-Fe_2O_3 is always formed and for highly substituted titanomaghemites the decomposition appears to take place in two steps as indicated by the two breaks in the log $\sigma = f(t)$ curves. In the first step α-Fe_2O_3 and TiO_2 are present and in the second step at $T > 900$ K pseudobrookite is formed in addition to α-Fe_2O_3.

References

1. B. GILLOT, F. JEMMALI, L. CLERC, AND A. ROUSSET, *React. Solids* **2,** 95 (1986).
2. B. GILLOT, F. JEMMALI, F. CHASSAGNEUX, C. SALVAING, AND A. ROUSSET, *J. Solid State Chem.* **45,** 317 (1982).
3. W. O'REILLY AND S. K. BANERJEE, *Nature (London)* **211,** 26 (1966).
4. P. W. READMAN AND W. O'REILLY, *Phys. Earth Planet. Inter.* **4,** 121 (1970).
5. R. FREER AND W. O'REILLY, *Mineral. Mag.* **43,** 889 (1980).
6. B. GILLOT, F. JEMMALI, AND A. ROUSSET, *Mater. Chem. Phys.* **15,** 577 (1986).
7. B. GILLOT, R. M. BENLOUCIF, AND F. JEMMALI, *J. Mater. Sci.* **19,** 3806 (1984).
8. V. KROPACEK AND M. LASTOVICKOVA, *J. Geophys.* **48,** 40 (1980).
9. A. TRESTMAN-MATTS, S. E. DORRIS, S. KUMARAKRISHNAN, AND T. O. MASON, *J. Amer. Ceram. Soc.* **66,** 829 (1983).
10. B. A. WECHSLER, D. H. LINDSLEY, AND C. T. PREWITT, *Amer. Mineral.* **69,** 754 (1984).
11. P. W. READMAN, *Phys. Earth Planet. Inter.* **16,** 196 (1978).
12. C. M. KEEFER AND P. N. SHIVE, *J. Geophys. Res.* **86,** 987 (1981).
13. B. GILLOT AND J. F. FERRIOT, *J. Phys. Chem. Solids* **37,** 857 (1976).
14. N. REZLESCU, *C. R. Acad. Sci. Paris Ser. II* **288,** 136 (1969).
15. B. GILLOT AND F. JEMMALI, *Phys. Status Solidi A* **76,** 601 (1983).
16. S. A. MAZEN AND B. A. SABRAH, *Thermochim. Acta* **105,** 1 (1986).
17. Z. HAUPTMAN, *Geophys. J.R. Astron. Soc.* **38,** 29 (1974).
18. S. D. JENSEN AND P. N. SHIVE, *J. Geophys. Res.* **78,** 8474 (1973).

19. B. GILLOT, R. M. BENLOUCIF, AND A. ROUSSET, *J. Phys. Chem. Solids* **42,** 209 (1981).
20. B. GILLOT AND F. BOUTON, *J. Solid State Chem.* **32,** 303 (1980).
21. K. S. RANE, A. K. NIKUMBA, AND A. J. MUKHEDKAR, *J. Mater. Sci.* **16,** 2387 (1981).
22. B. GILLOT, *Mater. Res. Bull.* **13,** 783 (1978).
23. T. NISHITANI, *Rock. Mag. Paleogeophys.* **6,** 128 (1979).
24. E. J. W. VERWEY, P. W. HAAJMAN, AND F. C. ROMEIJN, *J. Chem. Phys.* **15,** 181 (1947).
25. E. SCHMIDBAUER, *Phys. Chem. Miner.*, in press.
26. C. M. KEEFER AND P. N. SHIVE, *Earth Planet. Sci. Lett.* **51,** 199 (1980).